

# Impact of Spatial Filtering on Distortion from Low-Noise Amplifiers in Massive MIMO Base Stations

Christopher Mollén, Ulf Gustavsson, Thomas Eriksson, and Erik G. Larsson

**Abstract**—Because of the large number of antennas at the base station, the power consumption and cost of the low-noise amplifiers (LNAs) can be substantial. Therefore, we investigate the feasibility of inexpensive, power efficient LNAs, which inherently are less linear. To characterize the nonlinear distortion, the LNAs are described using a polynomial model, which allows for the derivation of the second-order statistics of the distortion. We show that some terms of the distortion from the LNAs combine coherently, and that the SINR of the symbol estimates therefore is limited by the linearity of the LNAs. Furthermore, the impact of a strong transmitter in the adjacent frequency band is investigated. The second-order statistics show how the power from that transmission leaks into the main band and interferes with the symbol estimates. The term that scales with the cube of the power received from the blocker can be filtered out by spatial processing. Only the coherent term that scales with the square of the power remains. Nonlinear distortion from the LNAs can be reduced by spatial processing in massive MIMO. However, it does not vanish as the number of antennas is increased.

**Index Terms**—amplifiers, antenna arrays, MIMO systems, nonlinear distortion, nonlinearities.

## I. INTRODUCTION

**L**OW-NOISE amplifiers (LNAs), which are used to amplify the weak received signal before further signal processing, are often assumed to be linear in the analysis of massive MIMO. Because of the great number of radio chains that are needed to build a massive MIMO base station, the power consumption of the hardware becomes an issue as the number of antennas is increased [2]. For example, the total power consumption of the many LNAs becomes significant, because their required output power does not decrease with the number of antennas, as is the case of the power amplifiers of the transmitter chain. To improve the power efficiency, the LNAs can be operated closer to saturation. Under such operation, however, the LNAs are nonlinear and the commonly made assumption on linearity is inaccurate. In this paper, we analyze how nonlinear LNAs would affect the decoding in a massive MIMO base station.

C. Mollén and E. Larsson are with the Department of Electrical Engineering, Linköping University, 581 83 Linköping, Sweden; e-mail: christopher.mollen@liu.se, erik.g.larsson@liu.se.

U. Gustavsson is with Ericsson Research, Gothenburg, Sweden; e-mail: ulf.gustavsson@ericsson.com.

T. Eriksson is with the Department of Electrical Engineering, Chalmers University of Technology, 412 96 Gothenburg, Sweden; e-mail: thomase@chalmers.se.

Parts of this work has been presented at the Asilomar Conference of Signals, Systems, and Computers [1].

This work was supported, in part, by Vetenskapsrådet (the Swedish research council) and ELLIIT. Parts of the work were done at the GHz Centre, which is sponsored by Vinnova.

In the downlink, it is known from analytical calculations [3], [4] and simulations [5] that power amplifier nonlinearities cause distortion that is correlated between antennas and, thus, adds up constructively in specific spatial directions. These spatial directions depend on the beamforming weights which, in turn, depend on the channel responses of the terminals targeted by the beamforming. This holds both for in-band distortion and out-of-band radiation.

Some studies of the effect of nonlinear amplification in the massive MIMO downlink employ a symbol-sampled discrete-time signal model [6], [7]. Such symbol-sampled signal models cannot accurately describe all effects of a nonlinearity on a continuous-time communication system, especially not phenomena that arise out-of-band, and do not accurately characterize the distortion.

It is important to note that models that describe the impact of hardware nonlinearities in terms of spatially uncorrelated extra additive noise [8] are not accurate, even though such models give correct final results for the in-band error vector magnitude in some cases [5]. Consistent with [9], behavioral models are used in this paper to describe the nonlinearities of the low-noise amplifiers. Furthermore, the system is described in continuous time. Hence, the spatial correlation of the distortion is accurately captured.

Recently, massive MIMO base stations with another kind of receiver nonlinearity—low-resolution ADCs—have received some attention [10]–[12]. In [13], [14], it was shown that the quantization distortion from low-resolution ADCs combines noncoherently when the channel has a high degree of frequency selectivity and the signal that is to be decoded is received with a small power compared to the interference and noise. However, in scenarios with frequency-flat channels and a single received signal with high SNR, the quantization distortion combines coherently. This is in line with the findings in this paper, which is natural since both an ADC and an LNA have finite dynamic ranges that lead to signal clipping.

The effect of nonlinear LNAs in massive MIMO has not yet been analyzed with a precise hardware model. The work in [15], [16] proposed a novel hardware architecture for the receiver in a massive MIMO base station that only employed a single LNA for the whole array. That work, however, used a simplistic hardware model that did not take nonlinear effects into account.

Here, we study the usual receiver architecture, where each antenna has its own LNA. We use a polynomial model to describe the nonlinear effects of the LNAs and use the Itô-

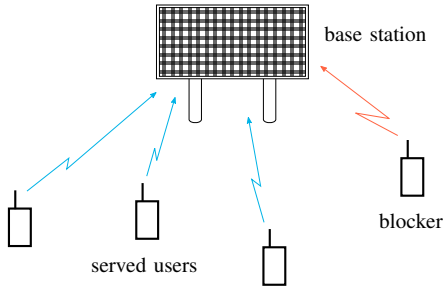


Fig. 1. The base station receives signals from multiple served users that are to be decoded. Additionally, it receives an interfering signal, which could be a signal from a user that is served by another base station or a signal from a malicious transmitter.

Hermite polynomials to derive the autocorrelation of the additional error term of the symbol estimate that is caused by the nonlinear LNAs. Further, we analyze the impact of a blocker—a strong transmitter in the adjacent frequency band—on the performance of the system.

We show that the distortion combines coherently, both in the presence and absence of a blocker, and that the received SINR is limited by the linearity of the LNAs. In the case of a blocker, it is shown that the nonlinear distortion causes two error terms: one that scales with the square of the received power from the blocker and one that scales with the cube of the received power. With sufficiently many antennas, spatial processing can remove the cube term. However, the square term has the same phases as the desired signal, and therefore combines coherently in the same way as the desired signal in the decoding.

## II. SYSTEM MODEL

The uplink transmission from  $K$  single-antenna users to a base station with  $M$  antennas is analyzed. Additionally, an undesired transmitter is considered, whose signal interferes with the received signals from the served users. The setting is depicted in Figure 1.

The transmitted signals are generated by pulse amplitude modulating discrete symbols with symbol period  $T$  and the pulse-shaping filter  $p(\tau)$ :

$$x_k(t) = \begin{cases} \sum_{n=-\infty}^{\infty} \sqrt{P_k} x_k[n] p(t - nT), & \text{if } k = 1, \dots, K, \\ \sum_{n=-\infty}^{\infty} \sqrt{P_k} x_k[n] p(t - nT) e^{j2\pi B t}, & \text{if } k = K + 1, \end{cases} \quad (1)$$

where  $k = 1, \dots, K$  are indices of served users and  $k = K + 1$  is the index of the blocker. The pulse-shaping filter is assumed to have bandwidth  $B$ , to be strictly limited to the frequency band  $[-B/2, B/2]$ . The power of the symbols is normalized such that  $\mathbb{E}[|x_k[n]|^2] = 1$  and  $\int_{-\infty}^{\infty} |p(\tau)|^2 d\tau = T$ , so that  $P_k$  represents the transmit power of transmitter  $k$ . The blocker is assumed to use the same pulse shape as the served users but transmits in the adjacent frequency band with center frequency  $f = B$ . The blocker could, for example, model a single-antenna user that belongs to another communication system that transmits in the right adjacent band.

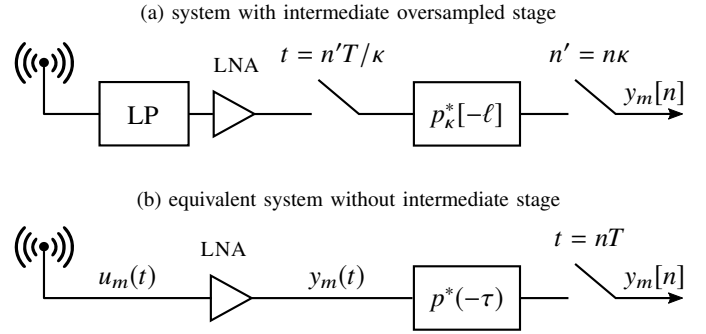


Fig. 2. The receiver model in (b) is equivalent to the model in (a) if the low-pass filter is zero outside  $[-\kappa/(2T), \kappa/(2T)]$  and  $p_\kappa[\ell] = p(\ell T/\kappa)$ .

The channel from transmitter  $k \in \{1, \dots, K + 1\}$  to base station antenna  $m$  is denoted by the coefficient  $h_{km} \in \mathbb{C}$ . Thus, the signal that is received at antenna  $m$  is given by:

$$u_m(t) = \sum_{k=1}^{K+1} h_{km} x_k(t) + z_m(t), \quad (2)$$

where  $z_m(t)$  is a stationary Gaussian process that is used to model the thermal noise of the receiver hardware. It will be assumed that the noise is independent across the antennas  $m$  and is white over the bandwidth of the three adjacent frequency bands. Specifically, it has constant power spectral density  $N_0$  over the band  $[-3B/2, 3B/2]$  and power spectral density equal to zero outside this bandwidth. The channel is assumed to be frequency flat in order to ease the notation. The extension to frequency-selective channels is tedious but straightforward.

In practice, this signal is converted into the digital receive signal  $y_m[n]$  via oversampling by a factor  $\kappa > 1$  as is shown in Figure 2 a. The intermediate oversampled stage is necessary, if the receive filter should be implemented as a digital filter, which allows for a precise filter design. However, the receiver chain shown in Figure 2 b, where the receive filter is implemented as an analog filter, is mathematically equivalent to the one in 2 a if: the anti-aliasing filter in front of the first sampling has a frequency response that is constant over the band of the receive filter, which is the same as the transmit filter  $[-B/2, B/2]$ , and the oversampling factor fulfills

$$\kappa > WT, \quad (3)$$

where  $W \geq B$  is the bandwidth of the anti-aliasing filter. If  $B = \alpha/T$ , where  $\alpha$  is the excess bandwidth, and if the anti-aliasing filter is constant over  $[-B/2, B/2]$  and zero outside  $[-3B/2, 3B/2]$ , then an oversampling factor  $\kappa \geq 3\alpha$  will ensure that (3) holds. If the excess bandwidth  $\alpha = 1.22$ , this means an oversampling factor  $\kappa \geq 4$  is sufficient. To simplify the exposition, we will therefore analyze the system in Figure 2 b without the intermediate oversampled stage.

Upon reception, the weak signal is amplified by an LNA. The operation of the LNA at antenna  $m$  will be denoted by  $\mathcal{A}_m$  and the amplified received signal is given by:

$$y_m(t) = \mathcal{A}_m(u_m(t)), \quad (4)$$

Note that, in full generality, the amplification operation  $\mathcal{A}_m$  is different at different antennas  $m$ .

The LNAS will be modeled as quasi-memoryless, i.e. as nonlinearities whose Volterra series have kernels that are constant, but possibly complex valued, over the frequency band of interest [17]. Such nonlinearities can be approximated arbitrarily well by a finite order polynomial model:

$$\mathcal{A}_m(u_m(t)) = \sum_{\varpi \leq \Pi: \text{odd}} b_{\varpi m} u_m(t) |u_m(t)|^{\varpi-1}, \quad (5)$$

where the sum is over all odd degrees  $\varpi = 1, 3, \dots, \Pi$  and  $\{b_{\varpi m}\}$  are complex coefficients. To facilitate a statistical analysis of the system, we rewrite the sum in (5) in terms of the Itô-Hermite polynomials  $H_{\varpi}(u)$ :

$$H_{\varpi}(u) \triangleq \sum_{n=0}^{\frac{\varpi-1}{2}} (-1)^n n! \binom{\frac{\varpi+1}{2}}{n} \binom{\frac{\varpi-1}{2}}{n} u |u|^{\varpi-1-2n}. \quad (6)$$

The amplified received signal is thus equivalently given by:

$$\mathcal{A}_m(u_m(t)) = \sum_{\varpi \leq \Pi: \text{odd}} a_{\varpi m} \sigma_{u_m}^{\varpi} H_{\varpi} \left( \frac{u_m(t)}{\sigma_{u_m}} \right), \quad (7)$$

where the complex coefficients  $\{a_{\varpi m}\}$  are linear combinations of the coefficients  $\{b_{\varpi m}\}$  and different powers of the signal power:

$$\sigma_{u_m}^2 = \mathbb{E} [|u_m(t)|^2]. \quad (8)$$

For example, if  $b_{m\varpi} = 0$  for all  $\varpi > 9$ , the Hermite coefficients are given by:

$$a_{1m} = b_{1m} + 2\sigma_{u_m}^2 b_{3m} + 6\sigma_{u_m}^4 b_{5m} + 24\sigma_{u_m}^6 b_{7m} + 120\sigma_{u_m}^8 b_{9m} \quad (9)$$

$$a_{3m} = b_{3m} + 6\sigma_{u_m}^2 b_{5m} + 36\sigma_{u_m}^4 b_{7m} + 240\sigma_{u_m}^6 b_{9m} \quad (10)$$

$$a_{5m} = b_{5m} + 12\sigma_{u_m}^2 b_{7m} + 120\sigma_{u_m}^4 b_{9m} \quad (11)$$

$$a_{7m} = b_{7m} + 20\sigma_{u_m}^2 b_{9m} \quad (12)$$

$$a_{9m} = b_{9m}. \quad (13)$$

It should be noted that  $\sigma_{u_m}^2$  depends on the time  $t$ , because the received signal  $u_m(t)$  is a cyclostationary signal. The Hermite coefficients  $\{a_{\varpi m}\}$  therefore also depend on  $t$ . For tractability, however, the dependence of the coefficients on time will be neglected, by replacing  $\sigma_{u_m}^2$  with the signal power  $\int_0^T \sigma_{u_m}^2 / T dt$  in (9)–(13). Many practical choices of pulses  $p(\tau)$  result in signals whose energy is evenly spread in time, especially those with a small excess bandwidth. For such pulses, it is a reasonable approximation to use constant Hermite coefficients. To obtain expressions that are valid for any pulse, it is straightforward to avoid the approximation by taking the dependency on time into consideration in what follows. However, the resulting expressions are less insightful as they will contain terms, in which the pulse and the coefficients are inseparable.

If the input signals are circularly symmetric and jointly complex Gaussian, the terms in the Hermite expansion are mutually orthogonal in the following sense. Let  $X$  and  $Y \sim \mathcal{CN}(0, 1)$  be two jointly Gaussian, circularly symmetric, complex random variables, then

$$\mathbb{E}[H_{\varpi}(X)H_{\varpi'}^*(Y)] = \left(\frac{\varpi+1}{2}\right)! \left(\frac{\varpi-1}{2}\right)! \mathbb{E}[XY^*] |\mathbb{E}[XY^*]|^{\varpi-1} \delta[\varpi - \varpi'], \quad (14)$$

where  $\delta[n] = 1$  when  $n = 0$  and  $\delta[n] = 0$  otherwise. Because of this property, the amplifier output, as given by the expansion in (7), is a sum of uncorrelated signals, each defined by:

$$u_{\varpi m}(t) \triangleq \sigma_{u_m}^{\varpi} H_{\varpi} \left( \frac{u_m(t)}{\sigma_{u_m}} \right). \quad (15)$$

It is noted that  $u_{1m}(t) = u_m(t)$ , because  $H_1(u) = u$ . The first term in the expansion (7) is thus the linear desired signal, and the rest of the terms represent uncorrelated distortion. We therefore partition the amplified signal into two components:

$$y_m(t) = a_{1m} u_m(t) + d_m(t), \quad (16)$$

where

$$d_m(t) \triangleq \sum_{3 \leq \varpi \leq \Pi: \text{odd}} a_{\varpi m} u_{\varpi m}(t). \quad (17)$$

In the symbol-sampled system model, the digital receive signal is obtained through demodulation with the matched filter  $p^*(-\tau)/T$ , which is scaled by the symbol period  $T$  to make the variance of the sampled noise

$$z_m[n] \triangleq \frac{1}{T} (p^*(-\tau) \star z_m(\tau))(nT) \sim \mathcal{CN}(0, N_0/T), \quad (18)$$

equal to  $N_0/T$ . The output of the matched filter is given by

$$\bar{y}_m(t) = \sum_{\varpi \leq \Pi: \text{odd}} a_{\varpi m} \bar{u}_{\varpi m}(t), \quad (19)$$

where the individual terms are given by

$$\bar{u}_{\varpi m}(t) = \frac{1}{T} (p^*(-\tau) \star u_{\varpi m}(\tau))(t). \quad (20)$$

The matched-filter output is then sampled:

$$y_m[n] = \bar{y}_m(nT) \quad (21)$$

$$= \sum_{\varpi \leq \Pi: \text{odd}} a_{\varpi m} \bar{u}_{\varpi m}(nT). \quad (22)$$

The signal part of the first term, the linear term, is denoted  $u_m[n] \triangleq \bar{u}_{1m}(nT)$ . The other terms, which represent the uncorrelated distortion, are denoted  $d_m[n] \triangleq y_m[n] - a_{1m} u_m[n]$ . If we assume perfect time synchronization, i.e. that the sampling instants are  $t = nT$  and that the pulse  $p(t)$  is a root-Nyquist pulse of parameter  $T$ , the linear part of the signal can be given as:

$$u_m[n] = \sum_{k=1}^K \sqrt{P_k} h_{km} x_k[n] + z_m[n]. \quad (23)$$

It is noted that the blocker does not affect this term because its signal and the receiver filter do not overlap in frequency. The channel will be assumed to be normalized, such that:

$$\mathbb{E} [|h_{km}|^2] = 1. \quad (24)$$

In this way, the power  $P_k$  is the received power from user  $k$ .

The estimate of the transmitted symbol of user  $k = 1, \dots, K$  is obtained by decoding the digital receive signal:

$$\hat{x}_k[n] \triangleq \sum_{m=1}^M w_{km} y_m[n] \quad (25)$$

$$= \sum_{m=1}^M a_{1m} w_{km} u_m[n] + \sum_{m=1}^M w_{km} d_m[n], \quad (26)$$

where  $\{w_{km}\}$  are the weights of the linear decoder of user  $k$ . The additional error in the estimate due to the nonlinear distortion is thus given by the last sum in (26):

$$e_k[n] \triangleq \sum_{m=1}^M w_{km} d_m[n]. \quad (27)$$

### III. EFFECT OF LNAS ON DECODING

From the expression for the symbol estimate in (26), it can be seen that the nonlinear LNAS affect the symbol estimates in two ways:

- 1) A multiplicative distortion of the decoding weights.
- 2) An additive distortion of the symbol estimates.

To evaluate these two effects, we will analyze the, so called, *use-and-forget bound* on the capacity.

*Theorem 1:* An achievable rate for the link in (26) is given by:

$$R_k = \log(1 + \text{SINR}_k), \quad (28)$$

where the effective SINR is given by:

$$\text{SINR}_k = \frac{|\mathbb{E}[\hat{x}_k[n]x_k^*[n]]|^2 / \mathbb{E}[|x_k[n]|^2]}{\mathbb{E}[|\hat{x}_k[n]|^2] - |\mathbb{E}[\hat{x}_k[n]x_k^*[n]]|^2 / \mathbb{E}[|x_k[n]|^2]} \quad (29)$$

The proof can be found in [18]. In the context of a nonlinear system, the use-and-forget bound is given by the following theorem.

*Corollary 1:* The effective SINR of a system with nonlinear LNAS is

$$\text{SINR}_k = \frac{P_k |g_k|^2}{\sum_{k'=1}^K P_{k'} I_{kk'} + MN_0/T + D}, \quad (30)$$

where the precoding gain is given by:

$$g_k = \sum_{m=1}^M \mathbb{E}[a_{1m} w_{km} h_{km}], \quad (31)$$

the interference from user  $k'$  to user  $k$  is:

$$I_{kk'} = \text{var} \left( \sum_{m=1}^M a_{1m} w_{km} h_{k'm} \right), \quad (32)$$

and the distortion variance

$$D \triangleq \text{var} \left( \sum_{m=1}^M w_{km} d_m[n] \right). \quad (33)$$

A system with perfectly linear LNAS, where all first-degree coefficients are equal,  $a_{1m} = 1$  for all  $m$ , and the distortion is zero,  $D = 0$ , is considered for comparison. When this system uses maximum-ratio decoding, i.e.  $w_{km} = a_{1m}^* h_{km}^*$ , and the channel is i.i.d. across  $m$  then the gain and interference are given by:

$$G_k \triangleq |g_k|^2 = \left| \sum_{m=1}^M \mathbb{E}[|h_{km}|^2] \right|^2 = M^2, \quad (34)$$

$$J_{kk'} \triangleq I_{kk'} = M \text{var}(h_{km}^* h_{k'm}). \quad (35)$$

If it is assumed that the fading is Gaussian, i.e. such that  $h_{km} \sim \mathcal{CN}(0, 1)$ , and the channel coefficients are independent across  $m$  and  $k$ , then the interference variances  $J_{kk'} = M$ .

While operation of the LNAS at a fixed point would be difficult in practice, we will assume that kind of operation for a moment, i.e. that the coefficients  $a_{1m}$ , which are functions of the received power, do not depend on the fading channel. Even if it might be difficult in practice, this mode of operation can be achieved approximately by varying the supply current to the amplifier to adjust for fading. Deterministic coefficients can also appear in a fading environment, where the energy of the channel is constant, such as in highly frequency-selective channels or in line-of-sight channels. If the LNA operation can be described by fixed gains  $\{a_{1m}\}$ , the effective SINR with nonlinear LNAS is given by the following theorem.

*Theorem 2:* In a system with LNAS whose first-degree coefficients  $\{a_{1m}\}$  are made constant and the channels  $\{h_{km}\}$  are identically distributed for all  $k$  and independent across  $m$ , the effective SINR of a maximum-ratio decoder  $w_{km} = a_{1m}^* h_{km}^*$  is given by:

$$\text{SINR} = \frac{\rho P_k G_k}{\sum_{k'=1}^K P_{k'} J_{kk'} + MN_0/T + D'}, \quad (36)$$

where the power loss due to variations in the power amplifier is

$$\rho \triangleq \frac{|\sum_{m=1}^M |a_{1m}|^2|^2}{M \sum_{m=1}^M |a_{1m}|^4}. \quad (37)$$

and the distortion power

$$D' \triangleq \frac{MD}{\sum_{m=1}^M |a_{1m}|^4}. \quad (38)$$

The proof of this theorem is given in the Appendix. Note that the power reduction  $\rho \leq 1$  due to the Cauchy-Schwarz inequality, with equality when all linear gains are the same,  $a_{1m} = a_{1m'}$  for all  $m$  and  $m'$ . Hence, differences in linearity between different amplifiers lead to a somewhat reduced decoding gain.

The phenomenon called *desensitization* [19, Ch. 2.1.1] can be observed in the gains  $\{a_{1m}\}$  of the desired linear part of the signal. In practical amplifiers, these gains grow smaller the higher power the input signal has. For example, from (9), it can be seen that a linearity of order  $\Pi = 3$  has the gain that is given by:

$$a_{1m} = b_{1m} + 2P_m^{\text{rx}} b_{3m}, \quad (39)$$

where  $P_m^{\text{rx}}$  is the received power at antenna  $m$ . To model an amplifier with transfer characteristics that saturate, the complex coefficients  $b_{1m}$  and  $b_{3m}$  have opposite phases, which normally is the case. Then the gain  $|a_{1m}|^2$  can become small if the received power  $P_m^{\text{rx}}$  is large.

In Figure 3, the gain is shown for different amounts of received powers for a specific amplifier. It can be observed that the desensitization effect can be significant. Even if it turns out that the distortion  $D'$  can be handled, desensitization will still have to be avoided if the LNAS are to be operated close to saturation.

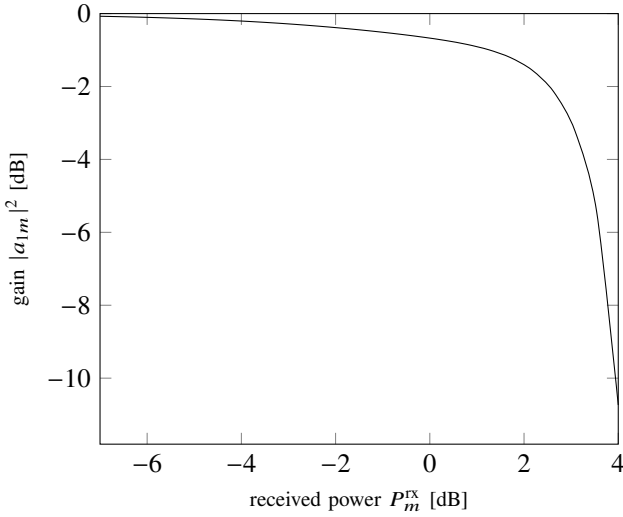


Fig. 3. Desensitization of the linear gain  $|a_{1m}|^2$  in an amplifier that is described by the polynomial coefficients  $b_{1m} = 1 - j0.00982$ ,  $b_{3m} = -0.00778 + j0.015$ ,  $b_{5m} = -0.026 - j0.00737$ ,  $b_{7m} = 0.00654 + j0.00166$  and  $b_{9m} = -0.000454 - j0.000114$  that are obtained from [20].

Since the desired signal, as well as the interference and the thermal noise, all are amplified by the linear gains given by  $\{|a_{1m}|^2\}$ , their relative powers do not change significantly by the desensitization. Desensitization however, increases the relative significance of the distortion, which is seen in (38), where the denominator  $\sum_{m=1}^M |a_{1m}|^4/M$  becomes small in case of desensitization.

Since the Hermite coefficients depend on the input power, which, in turn, depends on the channel fading, it is difficult to compute the use-and-forget bound in closed form in general. As described in Theorem 2, however, the overall effect of nonlinear LNAS is a lower decoding gain and extra additive distortion. The extra additive distortion will be studied in the following sections.

#### IV. SPECTRAL ANALYSIS OF SYMBOL ESTIMATES

To gain insight in how large the error due to the nonlinear distortion in (27) is, its second-order statistics will be analyzed using the correlation property of the Itô-Hermite polynomials.

Two cyclostationary signals  $x_1(t)$  and  $x_2(t)$  with period  $T$  have a cross-correlation function that is given by

$$R_{x_1 x_2}(t, \tau) \triangleq \mathbb{E}[x_1(t)x_2^*(t - \tau)] \quad (40)$$

that is periodic in the argument  $t$  with period  $T$ . By expanding the periodic cross-correlation function as a Fourier series, the cross-correlation of cycle index  $\alpha$  can be obtained as:

$$R_{x_1 x_2}^{(\alpha)}(\tau) \triangleq \frac{1}{T} \int_0^T R_{x_1 x_2}(t, \tau) e^{-j2\pi\alpha t/T} dt, \quad \alpha = 0, \pm 1, \pm 2, \dots \quad (41)$$

A good introduction to the second-order statistics of cyclostationary signals is given in [21]. Similarly, two weak-sense stationary, discrete signals  $y_1[n]$  and  $y_2[n]$  have a cross-correlation function that is given by

$$R_{y_1 y_2}[\ell] \triangleq \mathbb{E}[y_1[n]y_2^*[n - \ell]]. \quad (42)$$

The transmitted symbols are assumed to be independent and the cross-correlation function is therefore:

$$R_{s_k s_{k'}}[\ell] = \delta[k - k']\delta[\ell]. \quad (43)$$

It follows that the cyclostationary transmitted signals also are independent,  $R_{x_k x_{k'}}(t, \tau) = 0$  for  $k \neq k'$ , and their autocorrelation functions are given by:

$$R_{x_k x_k}(t, \tau) = \begin{cases} P_k \gamma(t, \tau) e^{-j2\pi B \tau}, & \text{if } k = K + 1, \\ P_k \gamma(t, \tau), & \text{otherwise,} \end{cases} \quad (44)$$

where the aggregate pulse is

$$\gamma(t, \tau) \triangleq \sum_{n=-\infty}^{\infty} p(t - nT) p^*(t - nT - \tau). \quad (45)$$

The cross-correlation of the received signals will then be:

$$R_{u_m u_{m'}}(t, \tau) = \sum_{k=1}^{K+1} h_{km} h_{km'}^* R_{x_k x_k}(t, \tau). \quad (46)$$

Note that the channel is treated as deterministic, since we are analyzing the signal for a given channel realization. Using the orthogonality property of the Hermite expansion in (14) of the amplifiers  $\mathcal{A}_m$ , the cross-correlation of the output signals is

$$R_{y_m y_{m'}}(t, \tau) = a_{1m} a_{1m'}^* R_{u_m u_{m'}}(t, \tau) + R_{d_m d_{m'}}(t, \tau), \quad (47)$$

where the cross-correlation of the distortion is:

$$\begin{aligned} R_{d_m d_{m'}}(t, \tau) &= \sum_{3 \leq \varpi \leq \Pi: \text{odd}} a_{\varpi m} a_{\varpi m'}^* R_{u_{\varpi m} u_{\varpi m'}}(t, \tau), \quad (48) \\ R_{u_{\varpi m} u_{\varpi m'}}(t, \tau) &\triangleq \left(\frac{\varpi + 1}{2}\right)! \left(\frac{\varpi - 1}{2}\right)! \\ &\quad \times R_{u_m u_{m'}}(t, \tau) |R_{u_m u_{m'}}(t, \tau)|^{\varpi-1}. \end{aligned} \quad (49)$$

The amplified received signal is filtered through a filter with impulse response  $p^*(-\tau)/T$  prior to sampling. The cross-correlation of cycle index  $\alpha$  of the terms in (20) is:

$$R_{\bar{u}_{\varpi m} \bar{u}_{\varpi m'}}^{(\alpha)}(\tau) = \frac{1}{T^2} \left( R_{u_{\varpi m} u_{\varpi m'}}^{(\alpha)}(t) \star \gamma^{(\alpha)}(t) \right)(\tau), \quad (50)$$

where the cross-correlations of cycle index  $\alpha$  of the input signal and the aggregate pulse are given, as in (41), by:

$$R_{u_{\varpi m} u_{\varpi m'}}^{(\alpha)}(\tau) = \frac{1}{T} \int_0^T R_{u_{\varpi m} u_{\varpi m'}}(t, \tau) e^{-j2\pi\alpha t/T} dt, \quad (51)$$

$$\gamma^{(\alpha)}(\tau) \triangleq \frac{1}{T} \int_0^T \gamma(t, \tau) e^{-j2\pi\alpha t/T} dt \quad (52)$$

$$= \frac{1}{T} \left( p^*(-t) \star p(t) e^{-j2\pi\alpha t/T} \right)(\tau). \quad (53)$$

The filter output is then sampled to produce the discrete-time signal  $u_{\varpi m}[n] \triangleq \bar{u}_{\varpi m}(t_0 + nT)$ . Since the sampling period  $T$  is equal to the period of the cyclostationary continuous-time signal, the discrete-time signal is a weak-sense stationary signal with cross-correlation:

$$R_{u_{\varpi m} u_{\varpi m'}}[\ell] = R_{\bar{u}_{\varpi m} \bar{u}_{\varpi m'}}(t_0 + nT, \ell T) \quad (54)$$

$$= R_{\bar{u}_{\varpi m} \bar{u}_{\varpi m'}}(t_0, \ell T) \quad (55)$$

$$= \sum_{\alpha=-\infty}^{\infty} R_{\bar{u}_{\varpi m} \bar{u}_{\varpi m'}}^{(\alpha)}(\ell T) e^{j2\pi\alpha t_0/T}. \quad (56)$$

TABLE I  
NUMBER OF TERMS AFFECTED BY BLOCKER

	$\nu =$	-1	0	1	2
# terms		$K^2$	$2K + K^3$	$1 + 2K^2$	$K$
# terms with $P_{K+1}^3$				1	
# terms with $P_{K+1}^2$			$2K$		$K$
# terms with $P_{K+1}$		$K^2$		$2K^2$	

In (55), the periodicity of the cross-correlation in its first argument was used. In (56), the periodic cross-correlation is expanded as a Fourier series. It is noted that the sampling offset in (21) was assumed to be  $t_0 = 0$ , which makes the complex exponentials in (56) equal to one for all  $\alpha$ .

### V. ANALYSIS OF THIRD-DEGREE DISTORTION

In order to derive some insights on the effect of the additive distortion on the decoding in an accessible way, the system is assumed to be noise-free, i.e.  $z_m(t) = 0, \forall m$ , and only the third-degree term of the distortion

$$d_m(t) = a_{3m}u_{3m}(t) \quad (57)$$

will be studied. In many practical scenarios, it is the third-degree term that causes the most distortion. The analysis of higher-degree terms can be done in a similar, albeit, more tedious way.

The cross-correlation of the third-degree distortion was given in (48) and (49) in terms of the third-degree cross-correlation of the received signal:

$$\begin{aligned} R_{u_{3m}u_{3m'}}(t, \tau) &= 2R_{u_m u_{m'}}(t, \tau)|R_{u_m u_{m'}}(t, \tau)|^2 \\ &= 2 \sum_{k=1}^{K+1} \sum_{k'=1}^{K+1} \sum_{k''=1}^{K+1} \bar{h}_{kk'k''m} \bar{h}_{kk'k''m'}^* P_k P_{k'} P_{k''} \gamma_{3,\nu}(kk'k'')(t, \tau), \end{aligned} \quad (58)$$

where the shorthand  $\bar{h}_{kk'k''m} \triangleq h_{km} h_{k'm} h_{k''m}^*$  was used and the third-degree pulse  $\gamma_{3,\nu}(t, \tau)$  is a frequency shifted version of the product  $\gamma(t, \tau)|\gamma(t, \tau)|^2$ :

$$\gamma_{3,\nu}(t, \tau) = \gamma(t, \tau)|\gamma(t, \tau)|^2 e^{j2\pi\nu B\tau}. \quad (60)$$

The frequency shift  $\nu B$  is a multiple of the carrier frequency of the blocker  $B$ . The multiplicity is determined by which of the indices  $k, k', k''$  that equals  $K+1$  (the index of the blocker) in the following way:

$$\nu(k, k', k'') \triangleq I(k) + I(k') - I(k'') \in \{-1, 0, 1, 2\}, \quad (61)$$

where  $I(k) = 1$  if  $k = K+1$  and  $I(k) = 0$  otherwise. In Table I, the number of terms in (59) belonging to a given frequency index  $\nu$  is shown together with the number of those terms that include different powers of the received power from the blocker. It is noted that, if the blocker is not present, all terms including  $P_{K+1} = 0$  disappear and only the  $K^3$  terms that belong to the pulse  $\gamma_{3,0}(t, \tau)$  are left.

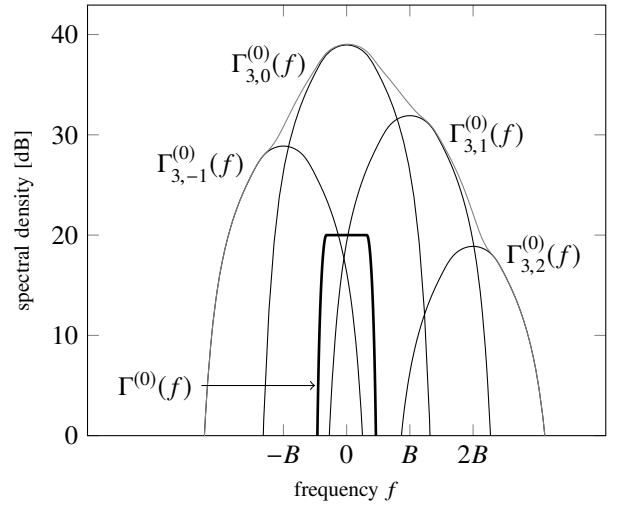


Fig. 4. The four pulse shapes in the sum in (59). The pulse  $p(\tau)$  has been chosen as a root-raised cosine with roll-off 0.22, and the Fourier transform  $\Gamma^{(0)}(f)$  of its ambiguity function at cycle index zero is shown for comparison. The pulses have been scaled by a factor equal to the number of terms corresponding to each pulse when there are  $K = 10$  served users, see Table I; this however is an arbitrary scaling. The sum of the pulses is shown in grey.

The cross-correlation of cycle index  $\alpha$  for the periodic correlation function in (59) is thus

$$R_{u_{3m}u_{3m'}}^{(\alpha)}(\tau) = 2 \sum_{k=1}^{K+1} \sum_{k'=1}^{K+1} \sum_{k''=1}^{K+1} \bar{h}_{kk'k''m} \bar{h}_{kk'k''m'}^* P_k P_{k'} P_{k''} \gamma_{3,\nu}(kk'k'')(\tau), \quad (62)$$

where the pulses are given by:

$$\gamma_{3,\nu}^{(\alpha)}(\tau) \triangleq \frac{1}{T} \int_0^T \gamma_{3,\nu}(t, \tau) e^{-j2\pi\alpha t/T} dt, \quad \nu = -1, 0, 1, 2. \quad (63)$$

The Fourier transforms  $\Gamma_{3,\nu}^{(0)}(f)$  of these pulses for  $\alpha = 0$  are shown in Figure 4. Three of these pulses overlap with the receive filter, so the cross-correlation of the matched-filtered signal will only contain these three pulses.

The cross-correlation of the matched-filtered and sampled signal that was given in (56) can now be written as:

$$\begin{aligned} R_{u_{3m}u_{3m'}}[\ell] &= a_{3m}a_{3m'}^* \sum_{\alpha=-\infty}^{\infty} \left( R_{u_{3m}u_{3m'}}^{(\alpha)}(\tau) \star \gamma^{(\alpha)}(\tau) \right) (\ell T) \\ &= a_{3m}a_{3m'}^* \sum_{k=1}^{K+1} \sum_{k'=1}^{K+1} \sum_{k''=1}^{K+1} \bar{h}_{kk'k''m} \bar{h}_{kk'k''m'}^* P_k P_{k'} P_{k''} \gamma_{3,\nu}(k, k', k'')[\ell] \end{aligned} \quad (64)$$

$$= a_{3m}a_{3m'}^* \sum_{\nu=-1}^2 \gamma_{3,\nu}[\ell] \sum_{(k,k',k'') \in \mathcal{K}_\nu} P_k P_{k'} P_{k''} \bar{h}_{kk'k''m} \bar{h}_{kk'k''m'}^*, \quad (65)$$

where the sets  $\mathcal{K}_\nu$  contain the user indices that affect a given pulse:

$$\mathcal{K}_\nu \triangleq \{(k, k', k'') : \nu(k, k', k'') = \nu\}. \quad (67)$$

and the three ambiguity functions are defined as follows:

$$\gamma_{3,\nu}[\ell] \triangleq \frac{1}{T^2} \sum_{\alpha=-\infty}^{\infty} \left( \gamma_{3,\nu}^{(\alpha)}(\tau) \star \gamma^{(\alpha)}(\tau) \right) (\ell T). \quad (68)$$

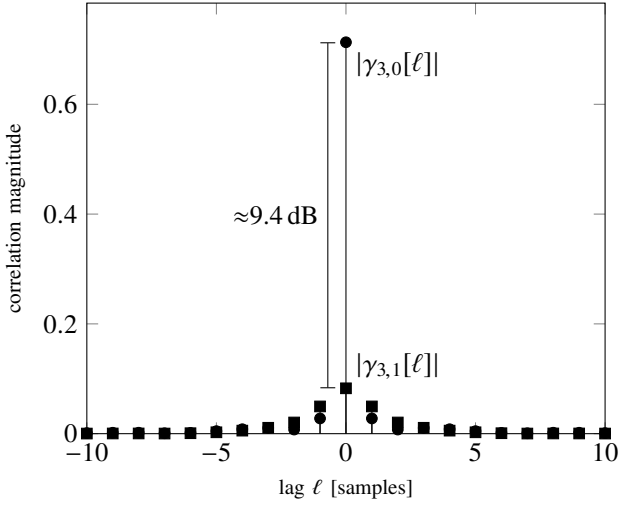


Fig. 5. The magnitude of the function  $|\gamma_{3,v}[\ell]|$  for  $v = 0, 1$ . The magnitude of  $|\gamma_{3,-1}[\ell]| = |\gamma_{3,1}[\ell]|$ . The pulse  $p(\tau)$  has been chosen as a root-raised cosine pulse with roll-off 0.22.

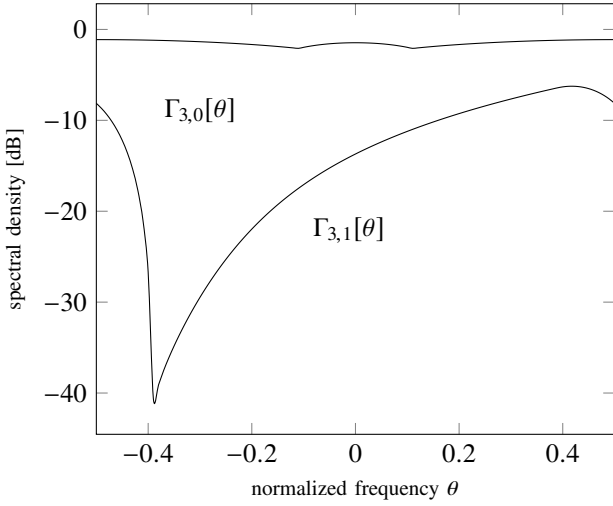


Fig. 6. The discrete-time Fourier transforms  $\Gamma_{3,v}[\theta]$  of the ambiguity functions  $\gamma_{3,v}[\ell]$ . Note that  $\Gamma_{3,-1}[\theta] = \Gamma_{3,1}[-\theta]$ .

Since the pulses  $\gamma^{(\alpha)}(\tau)$ , whose spectrum is limited to  $[-B/2, B/2]$  by construction, and  $\gamma_{3,2}(\tau)$  have disjoint supports in the frequency domain,  $\gamma_{3,2}[\ell] = 0$  for all  $\ell$ . The other three ambiguity functions can be seen in Figures 5 and 6 for a root-raised cosine pulse  $p(\tau)$  with roll-off 0.22. It can be seen that the center pulse  $\gamma_{3,0}[\ell]$  is practically frequency flat, while the adjacent pulses  $\gamma_{3,-1}[\ell]$  and  $\gamma_{3,1}[\ell]$  are frequency selective. The frequency content of these pulses mostly lies towards the low and high frequencies respectively, which means that distortion from these pulses can be avoided at certain frequencies.

From (66), it can be seen that the third-degree distortion term has a radiation pattern that is decided by the composite channels  $\{\bar{h}_{kk'k''m}, m = 1, \dots, M\}$ . If decoding is done as in (25), the distortion term will combine coherently for certain choices of  $\{w_{km}, m = 1, \dots, M\}$  and destructively for others. This is described by the autocorrelation function of the additive

distortion term  $e_k[n]$ :

$$\begin{aligned} R_{e_k e_k}[\ell] &= \sum_{m=1}^M \sum_{m'=1}^M w_{km} w_{km'}^* R_{u_{3m} u_{3m'}}[\ell] \\ &= \sum_{v=-1}^1 \gamma_{3,v}[\ell] \sum_{(k,k',k'') \in \mathcal{K}_v} P_k P_{k'} P_{k''} \\ &\quad \times \sum_{m=1}^M \sum_{m'=1}^M a_{3m} a_{3m'}^* \bar{h}_{kk'k''m} \bar{h}_{kk'k''m'}^* w_{km} w_{km'}^* \end{aligned} \quad (69)$$

The following observations can be made from (70):

- The distortion combines constructively in the directions given by

$$\{a_{3m} \bar{h}_{kk'k''m}, m = 1, \dots, M\} \quad (71)$$

for  $k, k', k'' = 1, \dots, K$ , which means that the decoding weights  $w_{km} = a_{3m} \bar{h}_{kk'k''m}^*$  will result in an increased amount of distortion.

- The number of directions  $\{a_{3m} \bar{h}_{kk'k''m}, m = 1, \dots, M\}$  is proportional to  $K^3$ . Note that the number only is *proportional* to  $K^3$ , because some of the directions are the same, e.g.  $\bar{h}_{kk'k''m} = \bar{h}_{kk'k''m}$ . When the number of directions is greater than the dimension of the signal space, which is  $M$ , the distortion can be isotropic, if all directions have the same power  $P_k P_{k'} P_{k''}$ . In this case, the distortion is picked up by any choice of decoding weights  $\{w_{km}\}$ .

## VI. LINE-OF-SIGHT AND MAXIMUM-RATIO DECODING

To obtain more intuition into how the distortion affects the decoding, a special case will be investigated in this section. It is assumed that the array is a uniform linear array, that the propagation is in line-of-sight and that maximum-ratio decoding is used. That means the frequency-flat channel to user  $k$  that is located at an angle  $\theta_k$  relative to the broadside of the array with antenna spacing  $\Delta$  is given by:

$$h_{km} = e^{jm\phi_k}, \quad (72)$$

where  $\phi_k \triangleq -2\pi \sin(\theta_k)\Delta/\lambda$  is the normalized sine angle of the incident signal and  $\lambda = c/f_c$  is the wavelength of the signal at the carrier frequency  $f_c$ . Using this notation, the composite channel becomes:

$$\bar{h}_{kk'k''m} = e^{jm(\phi_k + \phi_{k'} - \phi_{k''})}. \quad (73)$$

Since the modulus of all channel coefficients is the same, the received energy at all antennas will be the same. This means that the Hermite coefficients  $\{a_{3m}\}$  are the same for all  $m$  if all employed amplifiers are identical. To emphasize this, the index is dropped:  $a_3 \triangleq a_{3m}$ .

It is also assumed that maximum-ratio decoding is done, i.e. that

$$w_{km} = a_{1m}^* h_{km}^*, \quad \forall k, m. \quad (74)$$

Just like the third-order coefficients are independent of the antenna index  $m$ , the first-order coefficients  $\{a_{1m}\}$  are too. For notational simplicity, it will be assumed that  $a_{1m} = 1$  for all  $m$  without loss of generality.

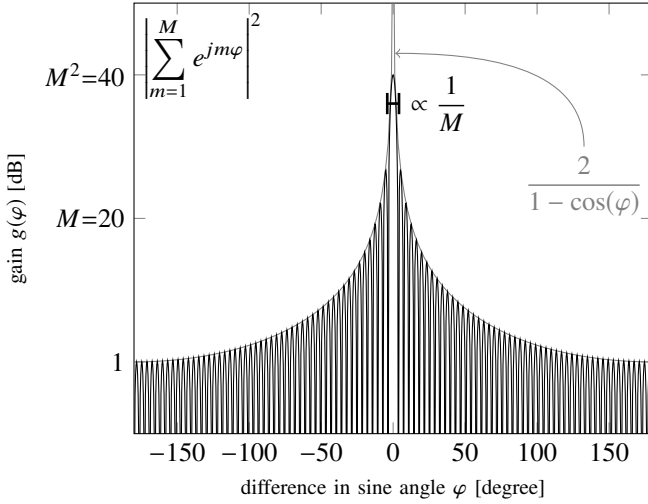


Fig. 7. The double sum in (77) is approximately zero, except when  $\varphi$  is close to zero. At  $\varphi = 0$ , the sum is equal to  $M^2$ . Here the sum is evaluated for  $M = 100$ .

In this case, the inner sum in (70) becomes

$$\sum_{m=1}^M \sum_{m'=1}^M a_{3m} a_{3m'}^* \bar{h}_{k'k''k'''} \bar{h}_{k'k''k'''}^* w_{km} w_{km'}^* \quad (75)$$

$$= |a_3|^2 \sum_{m=1}^M \sum_{m'=1}^M \bar{h}_{k'k''k'''} \bar{h}_{k'k''k'''}^* h_{km}^* h_{km'} \quad (76)$$

$$= |a_3|^2 \sum_{m=1}^M \sum_{m'=1}^M e^{j(m-m')(\phi_{k'} + \phi_{k''} - \phi_{k'''} - \phi_k)}. \quad (77)$$

$$= |a_3|^2 g(\phi_{k'} + \phi_{k''} - \phi_{k'''} - \phi_k), \quad (78)$$

where the double sum has been denoted by:

$$g(\varphi) \triangleq \sum_{m=1}^M \sum_{m'=1}^M e^{j(m-m')\varphi} = \left| \sum_{m=1}^M e^{jm\varphi} \right|^2. \quad (79)$$

The factor  $g(\phi_{k'} + \phi_{k''} - \phi_{k'''} - \phi_k)$  will be referred to as the *array gain* of the  $(k', k'', k''')$ -th term in (70). The array gain for different phase differences  $\varphi$  is shown in Figure 7 for  $M = 100$ . It can be observed that the array gain has the following properties:

- It has a main lobe around  $\varphi = 0$  of width  $2\pi/M$ .
- It has a maximum at  $\varphi = 0$ , where  $g(0) = M^2$ .
- Its envelope is upper bounded by:

$$g(\varphi) \leq \psi(\varphi) \triangleq \frac{2}{1 - \cos(\varphi)}. \quad (80)$$

- Because of (80),  $g(\varphi)$  stays finite when  $M$  grows for all  $\varphi$  except  $\varphi = 0$ , because  $g(0) = M^2$  that grows without bound.

The upper bound (80) can be used to show that  $g(\varphi)/M^2 < -20$  dB for all sine angle differences  $|\varphi| \in [12^\circ, 180^\circ]$  when there are  $M = 100$  antennas.

The autocorrelation of the error due to the distortion,

$$R_{e_k e_k}[\ell] = |a_3|^2 \sum_{v=-1}^1 \gamma_{3,v}[\ell] \sum_{(k,k',k'') \in \mathcal{K}_v} P_{k'} P_{k''} P_{k'''} g(\phi_{k'} + \phi_{k''} - \phi_{k'''} - \phi_k), \quad (81)$$

TABLE II

DOMINANT TERMS IN THE AUTOCORRELATION  $R_{e_1 e_1}[\ell]$  IN THE PRESENCE OF A BLOCKER, WHOSE RECEIVED POWER IS  $P_2$ , IN A LINE-OF-SIGHT SCENARIO WITH ONE SERVED USER, WHOSE RECEIVED POWER IS  $P_1$ .

	few antennas $M^2 \ll P_2/P_1$	many antennas $M^2 \gg P_2/P_1$
negligible blocker $P_1 \gg P_2$	$ a_3 ^2 \gamma_{3,0}[\ell] P_1^3 M^2$	$ a_3 ^2 \gamma_{3,0}[\ell] P_1^3 M^2$
strong blocker $P_1 \ll P_2$	$2 a_3 ^2 \gamma_{3,0}[\ell] P_1 P_2^2 M^2 +  a_3 ^2 \gamma_{3,1}[\ell] P_2^3 g(\phi_2 - \phi_1)$	$ a_3 ^2 \gamma_{3,0}[\ell] P_1 P_2^2 M^2$

will now be studied in a series of case studies, to illustrate how the distortion affects different system setups.

#### A. One User, One Blocker

In the case there is only one served user  $K = 1$ , index sets of the three frequencies  $v = -1, 0, 1$  are

$$\mathcal{K}_{-1} = \{(1, 1, 2)\} \quad (82)$$

$$\mathcal{K}_0 = \{(1, 1, 1), (2, 1, 2), (1, 2, 2)\} \quad (83)$$

$$\mathcal{K}_1 = \{(2, 1, 1), (1, 2, 1), (2, 2, 2)\}, \quad (84)$$

and the autocorrelation of the error due to the distortion becomes:

$$R_{e_k e_k}[\ell] = |a_3|^2 \left( \gamma_{3,-1}[\ell] P_1^2 P_2 g(\phi_1 - \phi_2) + \gamma_{3,0}[\ell] (P_1^3 + 2P_1 P_2^2) M^2 + \gamma_{3,1}[\ell] (2P_1^2 P_2 + P_2^3) g(\phi_2 - \phi_1) \right) \quad (85)$$

Depending on the relative powers between the user and the blocker and the number of antennas, only a few of these terms are significant. In Table II, four scenarios are specified: few or many antennas, weak or strong blocker. It is interesting to note that in all cases there is at least one term that combines coherently and thus scales with the number of antennas. These terms combine coherently because they have the same spatial correlation as the in-band signal. In other words, the error and the in-band signal will obtain the same array gain and the SINR of the estimate will remain finite also when the number of antennas grows large.

When the blocker is negligible, the autocorrelation is dominated by the  $P_1^3$  term,

$$R_{e_1 e_1}[\ell] \approx |a_3|^2 \gamma_{3,0}[\ell] P_1^3 M^2, \quad (86)$$

which is temporally white. As this term grows with the number of antennas, it remains when the number of antennas is increased—the distortion is *not* alleviated by the large number of antennas in massive MIMO.

When the blocker is strong, the autocorrelation function of the error is approximately:

$$R_{e_1 e_1}[\ell] \approx |a_3|^2 \left( 2\gamma_{3,0}[\ell] P_1 P_2^2 M^2 + \gamma_{3,1}[\ell] P_2^3 g(\phi_2 - \phi_1) \right). \quad (87)$$

The second term scales with  $P_2^3$  and can possibly hurt the performance of the system significantly if  $P_2$  is large. The first term only scales with  $P_2^2$ , but it also combines coherently and

scales with the number of antennas. Hence, if the number of antennas is increased and the difference in sine angles between the blocker and the user is outside the narrow main lobe,  $2\pi/M < |\phi_2 - \phi_1| \bmod 2\pi$ , the attenuation  $g(\phi_2 - \phi_1)$  goes to zero and the second term vanishes. However, if the blocker stands such that its sine angle is inside the narrow main lobe of the user,  $2\pi/M > |\phi_2 - \phi_1| \bmod 2\pi$ , then  $g(\phi_2 - \phi_1) \propto M^2$  and the second term does not vanish. In case of a strong blocker, the large number of antennas in massive MIMO thus *can* alleviate the distortion by reducing the distortion power from being proportional to  $P_2^3$  to being proportional to  $P_2^2$ .

### B. Multiple Users, No Dominant User

A user  $\chi$  is said to be *dominant* if the received power  $P_\chi \gg P_k$ , for all other users  $k \neq \chi$ . In this section, a case is considered, where the system performs power control, such that there is no dominant user. Furthermore, it is assumed that there is no blocker and that the number of antennas is large. Then many of the gains  $g(\cdot)$  in the sum (78) can be assumed to be negligibly small for a user  $k$  that has a unique angle of arrival, i.e. a  $\phi_k \neq \phi_{k'}$  for  $k' \neq k$ . Subsequently, only  $2(K-1)$  terms combine coherently, i.e. have  $g(\cdot) = M^2$ , and the autocorrelation can be approximated as follows:

$$R_{e_k e_k}[\ell] = |a_3|^2 \gamma_{3,0}[\ell] \sum_{(k', k'', k''') \in \mathcal{K}_0} P_{k'} P_{k''} P_{k'''} g(\phi_{k'} + \phi_{k''} - \phi_{k'''} - \phi_k) \quad (88)$$

$$\approx 2|a_3|^2 \gamma_{3,0}[\ell] \left( P_k^3 + 2P_k \sum_{k' \neq k} P_{k'}^2 \right) M^2. \quad (89)$$

It is noted that the power of the error grows with the number of users, because the total received power grows with the number of users. This stands in contrast to the amplifier induced distortion in the downlink, where the power of each user is proportional to  $1/K$  and the coherent distortion scales inversely with the number of users [3].

### C. Multiple Users, One Dominant User

If there is no power control in the system, the served users might be received with widely different powers. To illustrate this case, it will be assumed that one served user  $\chi$  is dominant,  $P_\chi \gg P_{k'}, \forall k' \neq \chi$ . The significant terms in the autocorrelation of the distortion error are then the terms that contain the third power of the power of the dominant user  $P_\chi^3$  and the terms with a large  $g(\cdot)$  that contain the power  $P_\chi$ . Just like in the single-user case, the autocorrelation of the dominant user is approximately:

$$R_{e_\chi e_\chi}[\ell] \approx |a_3|^2 \gamma_{3,0}[\ell] P_\chi^3 M^2. \quad (90)$$

For the other, non-dominant users,  $k \neq \chi$ , the autocorrelation is

$$R_{e_k e_k}[\ell] \approx |a_3|^2 \gamma_{3,0}[\ell] \left( P_\chi^3 g(\phi_\chi - \phi_k) + 2M^2 P_k P_\chi^2 \right). \quad (91)$$

If the dominant user has a different incidence angle,  $\phi_\chi \neq \phi_k$ , using a large number of antennas thus removes the first term that scales with  $P_\chi^3$ . The second term that scales with  $P_\chi^2$  combines coherently, however, and will not vanish with an increased number of antennas.

### D. Multiple Users, One Blocker

If there is a blocker that is received with a much higher power than the served users,  $P_{K+1}^2 \gg \sum_{k=1}^K P_k^2$ , then the autocorrelation of the distortion error will contain only a few significant terms, just as in the single-user case in (87). The terms containing the third power of the received power from the blocker  $P_{K+1}^3$  and the terms that combine coherently and contain the second power  $P_{K+1}^2$  are significant, and the autocorrelation is approximately:

$$R_{e_k e_k}[\ell] \approx |a_3|^2 \left( 2\gamma_{3,0}[\ell] P_{K+1}^2 P_k M^2 + \gamma_{3,1}[\ell] P_{K+1}^3 g(\phi_{K+1} - \phi_k) \right). \quad (92)$$

If the user has an incidence angle that is different from the blocker, the second term that scales with  $P_{K+1}^3$  becomes negligible when the number of antennas is increased. The first term that scales with  $P_{K+1}^2$ , however, remains as it combines coherently.

If the blocker stands inside the main lobe of the served user  $k$ ,  $2\pi/M > |\phi_{K+1} - \phi_k| \bmod 2\pi$ , both terms in (92) will combine coherently and the autocorrelation is:

$$R_{e_k e_k}[\ell] \approx |a_3|^2 M^2 \left( 2\gamma_{3,0}[\ell] P_{K+1}^2 P_k + \gamma_{3,1}[\ell] P_{K+1}^3 \right). \quad (93)$$

The second term that has a temporal correlation that is colored is the larger of the two terms if  $P_{K+1} > 2P_k \gamma_{3,0}[0]/\gamma_{3,1}[\ell]$ .

## VII. DIFFERENT AMPLIFIERS

Due to fabrication imperfections, the amplifiers might not all be equal. If that is the case, the array gain of the distortion is reduced. It is noted that the array gain of the desired linearly amplified signal is not significantly affected by variations among the amplifiers, because channel estimation adjusts for differences in the first-order coefficients  $\{a_{1m}\}$ . Hence, a reduction in the array gain of the distortion is not necessarily accompanied by a reduction in decoding gain of the symbol estimates. Variations among amplifiers would therefore possibly improve the effective SINR of the estimates.

If maximum-ratio decoding is employed and the weights

$$w_{km} = a_{1m}^* h_{km}^* \quad (94)$$

are used in (75), the array gain of the distortion becomes:

$$G(\varphi) \triangleq \left| \sum_{m=1}^M a_{3m} a_{1m}^* e^{jm\varphi} \right|^2. \quad (95)$$

To study how much the array gain of the distortion is reduced, the variations between the amplifiers are modeled as independent random deviations  $\alpha_m \sim \mathcal{CN}(0, \eta|a_3|^2)$  from a common mean  $\sqrt{1-\eta}a_3$ :

$$a_{3m} a_{1m}^* = \sqrt{1-\eta}a_3 + \alpha_m, \quad (96)$$

where the parameter  $0 \leq \eta \leq 1$  describes the degree of deviation between the amplifiers.

The array gain of the distortion is then random and becomes:

$$G(\varphi) = \left| \sum_{m=1}^M \sqrt{1-\eta}a_3 e^{jm\varphi} + \sum_{m=1}^M \alpha_m e^{jm\varphi} \right|^2. \quad (97)$$

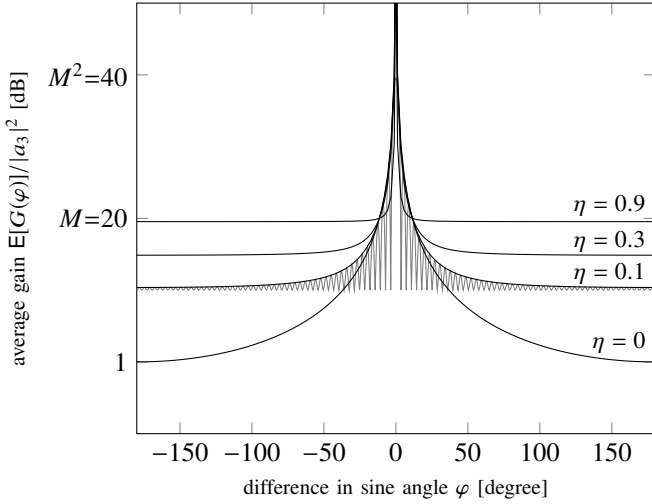


Fig. 8. Envelope of the mean array gain of the distortion in arrays with variable low-noise amplifiers and  $M = 100$  antennas. Around  $\varphi = 0$  the gain is finite and is not visible from the envelope. The array gain at  $\varphi = 0$  is shown in Figure 9. The mean array gain of the distortion is shown for  $\eta = 0.1$  in grey.

The expectation of this random array gain is:

$$\mathbb{E}[G(\varphi)] = (1 - \eta)|a_3|^2 g(\varphi) + M\eta|a_3|^2 \quad (98)$$

$$= |a_3|^2 (g(\varphi)(1 - \eta) + M\eta). \quad (99)$$

The expectation in (99) is shown in Figure 8, where the  $g(\varphi)$  is upper bounded by its envelope  $\psi(\varphi)$ . It can be seen that the suppression ability at  $\varphi \neq 0$  degrades when the degree of deviation  $\eta$  increases.

The average array gain of terms that combine coherently is given by the expectation of the array gain at  $\varphi = 0$ :

$$\mathbb{E}[G(0)] = |a_3|^2 M^2 (1 - \eta(1 - 1/M)). \quad (100)$$

This expectation is shown in Figure 9. It can be seen how the array gain of the distortion that combines coherently decreases with an increasing degree of deviation  $\eta$  among the amplifiers. However, the decrease is small and, not until  $\eta$  is close to one, the array gain becomes significantly lower than the case of identical amplifiers.

Deviations between amplifiers thus somewhat decrease the array gain of the coherent distortion. At the same time, the deviations also decrease the suppression ability of noncoherent distortion, and effectively increase the noncoherent part of the distortion.

## VIII. CONCLUSION

The uncorrelated-distortion model popularized in [22] is not physically correct and can yield totally wrong conclusions in many cases of practical interest. We show how nonlinear LNAs create correlated additive distortion that combines coherently in massive MIMO systems. The effect limits the effective SINR that can be achieved when the number of antennas is increased. In the case of a single served user in line-of-sight, all the distortion combines coherently and the effect of the nonlinear LNAs is the same as in a SISO system without spatial processing. In other cases, however, some of the distortion is filtered out

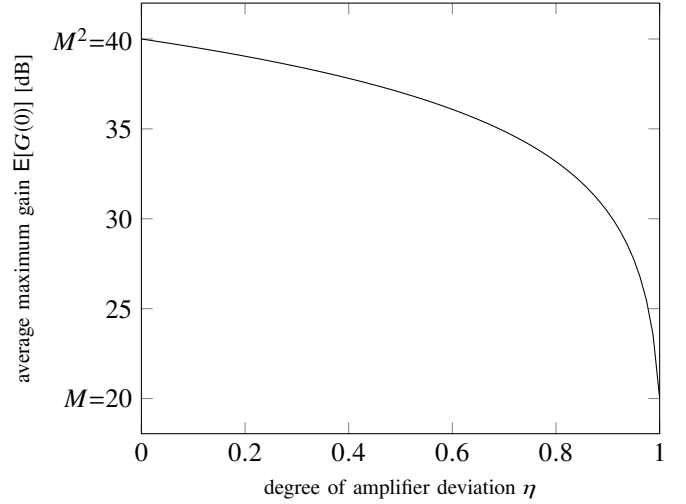


Fig. 9. The array gain of the distortion decreases the less the amplifier coefficients are alike. The curve is for  $M = 100$  antennas.

in the decoding, which makes the effect of the nonlinear LNAs smaller than in a SISO system. Specifically, in the presence of a blocker, the additional distortion that combines coherently grows only with the square of the received interfering power, instead of the cube, which is the case in systems without spatial processing.

## APPENDIX PROOF OF THEOREM 2

First the gain in (31) is investigated with  $w_{km} = h_{km}^*$ :

$$g_k = \sum_{m=1}^M |a_{1m}|^2 \mathbb{E}[|h_{km}|^2] \quad (101)$$

$$= \sum_{m=1}^M |a_{1m}|^2. \quad (102)$$

The square of this is  $|g_k|^2 = G_k |\sum_{m=1}^M |a_{1m}|^2|^2 / M^2$ .

Then the interference variance in (32) is considered:

$$I_{kk'} = \text{var} \left( \sum_{m=1}^M |a_{1m}|^2 h_{km}^* h_{k'm} \right) \quad (103)$$

$$= \sum_{m=1}^M |a_{1m}|^4 \text{var}(h_{km}^* h_{k'm}) \quad (104)$$

$$= J_{kk'} \frac{\sum_{m=1}^M |a_{1m}|^2}{M}, \quad (105)$$

because the channels are independent across  $m$ . Because the channel coefficients are identically distributed across  $m$ , the variances  $\text{var}(h_{km}^* h_{k'm})$  are equal for all  $m$ . The variance of the nonlinear system is therefore equal to the variance in (35) of the linear system:  $I_{kk'} = J_{kk'}$ .

Similarly, the noise term has the variance:

$$\text{var} \left( \sum_{m=1}^M |a_{1m}|^2 w_{km} z_m[n] \right) = \sum_{m=1}^M |a_{1m}|^4 \underbrace{\text{var}(w_{km} z_m[n])}_{=N_0/T} \quad (106)$$

$$= \frac{N_0}{T} \sum_{m=1}^M |a_{1m}|^4. \quad (107)$$

By normalizing this with respect to the total amplification  $\sum_{m=1}^M |a_{1m}|^2$  the noise variance is obtained and the theorem follows.

## REFERENCES

- [1] C. Mollén, U. Gustavsson, T. Eriksson, and E. G. Larsson, "Analysis of nonlinear low-noise amplifiers in massive MIMO base stations," in *Proc. Asilomar Conf. Signals, Syst., and Comput.*, Oct. 2017.
- [2] S. Buzzi, C.-L. I, T. E. Klein, H. V. Poor, C. Yang, and A. Zappone, "A survey of energy-efficient techniques for 5G networks and challenges ahead," *IEEE J. Sel. Areas Commun.*, vol. 34, no. 4, pp. 697–709, Apr. 2016.
- [3] C. Mollén, U. Gustavsson, T. Eriksson, and E. G. Larsson, "Spatial characteristics of distortion radiated from antenna arrays with transceiver nonlinearities," *ArXiv E-Print*, Nov. 2017, arXiv:1711.02439 [cs.IT].
- [4] C. Mollén, E. G. Larsson, U. Gustavsson, T. Eriksson, and R. W. Heath, Jr., "Out-of-band radiation from large antenna arrays," *ArXiv E-Print*, Nov. 2016, arxiv:1611.01359 [cs.IT]. [Online]. Available: <http://arxiv.org/abs/1611.01359>
- [5] U. Gustavsson, C. Sanchez Perez, T. Eriksson, F. Athley, G. Durisi, P. N. Landin, K. Hausmair, C. Fager, and L. Svensson, "On the impact of hardware impairments on massive MIMO," in *Proc. IEEE Global Commun. Conf.*, Dec. 2014.
- [6] S. Blandino, C. Desset, A. Bourdoux, L. V. der Perre, and S. Pollin, "Analysis of out-of-band interference from saturated power amplifiers in massive MIMO," in *Proc. Eur. Conf. Networks and Commun.*, Jun. 2017, pp. 1–6.
- [7] Y. Zou, O. Raesi, L. Antilla, A. Hakkarainen, J. Vieira, F. Tufvesson, Q. Cui, and M. Valkama, "Impact of power amplifier nonlinearities in multi-user massive MIMO downlink," in *IEEE Globecom Workshops*, Dec. 2015, pp. 1–7.
- [8] E. Björnson, J. Hoydis, M. Kountouris, and M. Debbah, "Massive MIMO systems with non-ideal hardware: Energy efficiency, estimation, and capacity limits," *IEEE Trans. Inf. Theory*, vol. 60, no. 11, pp. 7112–7139, Nov. 2014.
- [9] F. M. Ghannouchi and O. Hammi, "Behavioral modeling and predistortion," *IEEE Microw. Mag.*, vol. 10, no. 7, pp. 52–64, Dec. 2009.
- [10] D. Verenzuela, E. Björnson, and M. Matthaiou, "Hardware design and optimal ADC resolution for uplink massive MIMO systems," in *Proc. Sensor Array and Multichannel Signal Process. Workshop*. IEEE, Jul. 2016, pp. 1–5.
- [11] M. Sarajlić, L. Liu, and O. Edfors, "When are low resolution ADCs energy efficient in massive MIMO?" *IEEE Access*, vol. 5, pp. 14 837–14 853, Jul. 2017.
- [12] S. Jacobsson, G. Durisi, M. Coldrey, U. Gustavsson, and C. Studer, "Throughput analysis of massive MIMO uplink with low-resolution ADCs," *IEEE Trans. Wireless Commun.*, 2017.
- [13] C. Mollén, J. Choi, E. G. Larsson, and R. W. Heath, Jr., "Uplink performance of wideband massive MIMO with one-bit ADCs," *IEEE Trans. Wireless Commun.*, vol. 16, no. 1, pp. 87–100, Jan. 2017.
- [14] —, "Achievable uplink rates for massive MIMO with coarse quantization," in *Proc. IEEE Int. Conf. on Acoust., Speech and Signal Process.* IEEE, Mar. 2017, pp. 6488–6492.
- [15] P. Zhao, S. Bhattacharjee, J. H. Park, P. Subrahmanya, B. Banister, and M. Narasimha, "Energy-efficient power and LNA control for wireless multi-channel communication," in *wcnc*, Mar. 2017, pp. 1–6.
- [16] Z. Yu, C. Shen, P. Zhao, and X. Luo, "On energy efficient uplink multi-user MIMO with shared LNA control," *ArXiv E-Print*, Sep. 2017, arxiv:1709.06856 [cs.IT].
- [17] R. Raich and G. T. Zhou, "On the modeling of memory nonlinear effects of power amplifiers for communication applications," in *Proc. IEEE Digital Signal Process. Workshop*. IEEE, Oct. 2002, pp. 7–10.
- [18] T. L. Marzetta, E. G. Larsson, H. Yang, and H. Q. Ngo, *Fundamentals of Massive MIMO*. Cambridge University Press, 2016.
- [19] B. Razavi, *RF microelectronics*. Prentice Hall, 1998.
- [20] "Further elaboration on PA models for NR," [http://www.3gpp.org/ftp/tsg\\_ran/WG4\\_Radio/TSGR4\\_80/Docs/R4-165901.zip](http://www.3gpp.org/ftp/tsg_ran/WG4_Radio/TSGR4_80/Docs/R4-165901.zip), Ericsson AB, Tech. Rep. R4-165901, Aug. 2016, online: accessed 2017-03-20.
- [21] W. A. Gardner, A. Napolitano, and L. Paura, "Cyclostationarity: Half a century of research," *Signal Process.*, vol. 86, no. 4, pp. 639–697, Apr. 2006.
- [22] E. Björnson, J. Hoydis, M. Kountouris, and M. Debbah, "Massive MIMO systems with non-ideal hardware: Energy efficiency, estimation, and capacity limits," *IEEE Trans. Inf. Theory*, vol. 60, no. 11, pp. 7112–7139, Nov. 2014.